Article ID: 1671-3664(2003)01-0051-08

A seismic free field input model for FE-SBFE coupling in time domain

Yan Junyi(阎俊义)†, Jin Feng(金峰)‡, Xu Yanjie(徐艳杰)§,
Wang Guanglun(王光纶)‡ and Zhang Chuhan(张楚汉)‡

Department of Hydraulic Engineering, Tsinghua University, Beijing 100084, China

Abstract: A seismic free field input formulation of the coupling procedure of the finite element (FE) and the scaled boundary finite-element (SBFE) is proposed to perform the unbounded soil-structure interaction analysis in time domain. Based on the substructure technique, seismic excitation of the soil-structure system is represented by the free-field motion of an elastic half-space. To reduce the computational effort, the acceleration unit-impulse response function of the unbounded soil is decomposed into two functions: linear and residual. The latter converges to zero and can be truncated as required. With the prescribed tolerance parameter, the balance between accuracy and efficiency of the procedure can be controlled. The validity of the model is verified by the scattering analysis of a hemi-spherical canyon subjected to plane harmonic P, SV and SH wave incidence. Numerical results show that the new procedure is very efficient for seismic problems within a normal range of frequency. The coupling procedure presented herein can be applied to linear and nonlinear earthquake response analysis of practical structures which are built on unbounded soil.

Keywords: soil-structure interaction; scaled boundary finite-element; seismic excitation; time domain

1 Introduction

The seismic response of many practical engineering works, such as long span bridges, offshore structures, underground constructions, nuclear power plants, high dams, etc., is affected remarkably by the unbounded soil. To accommodate Sommerfeld's radiation conditions, many kinds of numerical procedures have been developed in the past three decades, including the boundary integral equation method or boundary element method, infinite element method and finite element method with various transmitting boundaries. In this regard, a novel procedure called the cloning algorithm was proposed by Dasgupta in 1982, in which the similarity-based formulation is used to satisfy the radiation conditions and the dynamic response of unbounded media is modeled in finite element sense. From then on, several similarity-based procedures were presented, such as the generalized cloning algorithm (Wolf and Weber, 1982), multi-cell cloning algorithm (Wolf and Song, 1994), the scaled boundary finite-element method (SBFE) alias consistent infinitesimal finite-element cell method (Wolf and Song, 1994; Song and Wolf, 1997) and forecasting method (Song and Wolf, 1995). As a development of the cloning algorithm, SBFE combines the advantages of both the finite-element method (FE) and boundary-element method (BE). On the one hand, only the boundary is discretized which leads to a reduction of the spatial dimension by one. On the other hand, no fundamental solution is required which implies a wider application scope compared with BE. As a semi-analytical algorithm, it is exact in the radial direction and converges to an exact solution in finite element sense in the circumferential direction. SBFE can be applied to static, diffusion and wave propagation problems both in frequency and time domains (Wolf and Song, 1996). Thus incorporating the SBFE with FE directly in the time domain to perform linear/nonlinear seismic analysis of the unbounded soil-structure system provides a very attractive procedure for this topic.

Recently, several combined models of FE and SBFE have been presented to perform the dynamic soil-structure interaction analysis. A three-dimensional coupling scheme is proposed in time domain by Zhang *et al.* (1999), in which the acceleration unit-impulse response function of the unbound soil is

Correspondence to: Zhang Chuhan, Dept. Hydraulic Eng., Tsinghua University, Beijing 100084, China
Tel: +8610-6278-3165
E-mail: zch-dhh@tsinghua.edu.cn
†Graduate Student; ‡Professor; § Associate Professor

Supported by: the National Key Basic Research and Development Program under Grant No. 2002CB412709
Received date: 2003-02-21; **Accepted date**: 2003-05-05

approximated by a piece-wise linear function to reduce the computational effort. However, with this approximation the accuracy of the procedure becomes uncontrollable, which reduces the primary advantage of the SBFE method. A frequency-based scheme was presented by Genes and Kocak (2002), where a parallel algorithm is introduced to solve the first order nonlinear ordinary differential equations for the dynamic stiffness matrix of the unbounded region. Combining the SBFE with the standard FE using Lagrange multipliers, Ekevid and Wiberg(2002) analyzed the wave propagation in solid materials under moving loads. To achieve high efficiency and accuracy controllability synchronously, a system-realization-based coupling procedure of FE-SBFE was proposed by Yan *et al.* (2002) and Yan *et al.* (2003), which is performed directly in time domain and where only the external time-varying loading is involved. In this paper, a seismic free field input formulation of the coupling procedure is presented and a more efficient scheme is used to evaluate the soil-structure interaction forces. High efficiency and precision controllability are still retained as primary advantages of the coupling scheme. The validity of the model is demonstrated by numerical examples.

2 Description of the coupling system

A typical soil-structure interaction system is shown in Fig. 1, where the practical structure, can be a reactor building, cooling tower, high-rise building etc. The structure comprising a part of the bounded adjacent foundation is viewed as a generalized structure (signed by s) which is discretized by FE permitting nonlinear behavior to occur, while the remaining unbounded ground (signed by g) is always selected as a linear motion and is modeled by SBFE. In time domain, the motion equation of the structure and the soil-structure interaction forces can be represented as

$$\begin{bmatrix} \boldsymbol{M}^{s}_{ss} & \boldsymbol{M}^{s}_{sb} \\ \boldsymbol{M}^{s}_{bs} & \boldsymbol{M}^{s}_{bb} \end{bmatrix} \begin{Bmatrix} \ddot{\boldsymbol{u}}_{s}(t) \\ \ddot{\boldsymbol{u}}_{b}(t) \end{Bmatrix} + \begin{bmatrix} \boldsymbol{C}^{s}_{ss} & \boldsymbol{C}^{s}_{sb} \\ \boldsymbol{C}^{s}_{bs} & \boldsymbol{C}^{s}_{bb} \end{bmatrix} \begin{Bmatrix} \dot{\boldsymbol{u}}_{s}(t) \\ \dot{\boldsymbol{u}}_{b}(t) \end{Bmatrix} +$$

$$\begin{bmatrix} \boldsymbol{K}^{s}_{ss} & \boldsymbol{K}^{s}_{sb} \\ \boldsymbol{K}^{s}_{bs} & \boldsymbol{K}^{s}_{bb} \end{bmatrix} \begin{Bmatrix} \boldsymbol{u}_{s}(t) \\ \boldsymbol{u}_{b}(t) \end{Bmatrix} = \begin{Bmatrix} \boldsymbol{p}_{s}(t) \\ -\boldsymbol{r}_{b}(t) \end{Bmatrix} \quad (1)$$

$$\boldsymbol{r}_{b}(t) = \int_{0}^{t} \boldsymbol{G}^{g}_{bb}(t-\tau)(\ddot{\boldsymbol{u}}_{b}(\tau) - \ddot{\boldsymbol{u}}^{g}_{b}(\tau))\mathrm{d}\tau \quad (2)$$

where $\boldsymbol{M}$, $\boldsymbol{C}$ and $\boldsymbol{K}$ are mass, damping and static-stiffness matrices of the structure respectively, $\boldsymbol{G}^{g}_{bb}$ is the acceleration unit-impulse response matrix of the unbounded soil; $\ddot{\boldsymbol{u}}^{g}_{b}$ is the scattered motion of the foundation without the structure which serves as the seismic input of the coupling system; $\boldsymbol{p}_{s}$ is the external loading vector and $\boldsymbol{r}_{b}$ is the interaction force vector. The superscripts s and g denote the generalized structure and the unbounded foundation, respectively, while the subscripts b and s stand for degrees of freadom of the nodes located on the structure-soil interface and those of the remaining nodes of the structure, respectively.

The interaction forces can be expressed as some functions of displacement, velocity and acceleration. Herein, the acceleration formulation rather than the displacement is used to avoid singularity.

$\boldsymbol{M}$, $\boldsymbol{C}$ and $\boldsymbol{K}$ can be obtained using finite element assemblage, and $\boldsymbol{G}^{g}_{bb}$ can be calculated via SBFE at distinct time stations. When seismic input motion $\ddot{\boldsymbol{u}}^{g}_{b}$ is determined, dynamic response of the coupling system can be evaluated from Eqs.(1) and (2) by using time integral scheme.

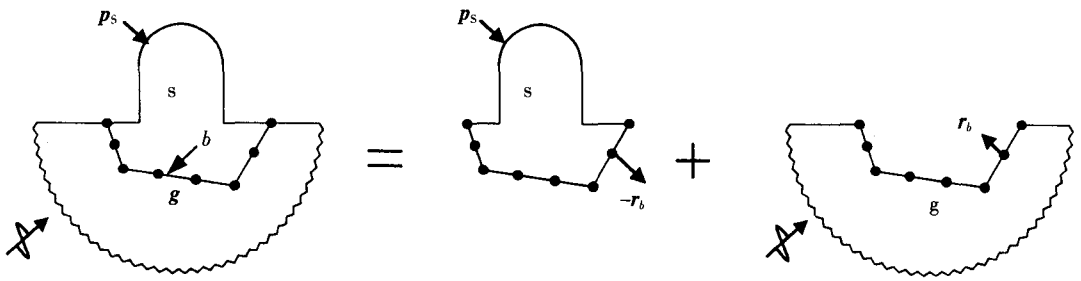

Fig. 1 A typical soil-structure interaction system

3 Seismic excitation input model

The scattering motion of the foundation $\ddot{\boldsymbol{u}}^{g}_{b}$ depends on the shape of excavation and is difficult to evaluate directly in time domain. Therefore, it is convenient to replace it with the free-field motion of the elastic half-space $\ddot{\boldsymbol{u}}^{f}_{b}$, which can be determined using many available procedures (Eringen and Suhubi, 1974; Wolf,

1985).

As shown in Fig. 2, a half-space can be considered as the combination of a finite excavation and the unbounded foundation mentioned in section 2. Similar to Eqs.(1) and (2), the motion equation of the finite excavation and the soil-excavation interaction forces can be represented in time domain as

$$\begin{bmatrix} \boldsymbol{M}^{\mathrm{e}}_{bb} & \boldsymbol{M}^{\mathrm{e}}_{be} \\ \boldsymbol{M}^{\mathrm{e}}_{eb} & \boldsymbol{M}^{\mathrm{e}}_{ee} \end{bmatrix} \begin{Bmatrix} \ddot{\boldsymbol{u}}^{\mathrm{f}}_{b}(t) \\ \ddot{\boldsymbol{u}}^{\mathrm{f}}_{e}(t) \end{Bmatrix} + \begin{bmatrix} \boldsymbol{C}^{\mathrm{e}}_{bb} & \boldsymbol{C}^{\mathrm{e}}_{be} \\ \boldsymbol{C}^{\mathrm{e}}_{eb} & \boldsymbol{C}^{\mathrm{e}}_{ee} \end{bmatrix} \begin{Bmatrix} \dot{\boldsymbol{u}}^{\mathrm{f}}_{b}(t) \\ \dot{\boldsymbol{u}}^{\mathrm{f}}_{e}(t) \end{Bmatrix} + \begin{bmatrix} \boldsymbol{K}^{\mathrm{e}}_{bb} & \boldsymbol{K}^{\mathrm{e}}_{be} \\ \boldsymbol{K}^{\mathrm{e}}_{eb} & \boldsymbol{K}^{\mathrm{e}}_{ee} \end{bmatrix} \begin{Bmatrix} \boldsymbol{u}^{\mathrm{f}}_{b}(t) \\ \boldsymbol{u}^{\mathrm{f}}_{e}(t) \end{Bmatrix} = \begin{Bmatrix} -\boldsymbol{r}^{\mathrm{f}}_{b}(t) \\ \boldsymbol{0} \end{Bmatrix} \tag{3}$$

$$\boldsymbol{r}^{\mathrm{f}}_{b}(t) = \int_0^t \boldsymbol{G}^{\mathrm{g}}_{bb}(t-\tau)(\ddot{\boldsymbol{u}}^{\mathrm{f}}_{b}(\tau) - \ddot{\boldsymbol{u}}^{\mathrm{g}}_{b}(\tau))\mathrm{d}\tau \tag{4}$$

where $\boldsymbol{r}^{\mathrm{f}}_{b}$ is the soil-excavation interaction force vector. The superscript e indicates excavation and the subscript e indicates the degrees of freedom of the excavation nodes, excluding those on the interface.

Subtracting Eq. (4) from Eq. (2) and eliminating the term $\ddot{\boldsymbol{u}}^{\mathrm{g}}_{b}$, the soil-structure interaction force can be rewritten as

$$\boldsymbol{r}_{b}(t) = \int_0^t \boldsymbol{G}^{\mathrm{g}}_{bb}(t-\tau)(\ddot{\boldsymbol{u}}_{b}(\tau) - \ddot{\boldsymbol{u}}^{\mathrm{f}}_{b}(\tau))\mathrm{d}\tau + \boldsymbol{r}^{\mathrm{f}}_{b}(t) \tag{5}$$

When the finite excavation is discretized by **FE**, the property matrices can be obtained by standard assemblage and then $\boldsymbol{r}^{\mathrm{f}}_{b}$ can be evaluated straightforwardly through Eq. (3). Finally, substituting Eq. (5) into Eq. (1), the seismic response of the coupling system can be obtained.

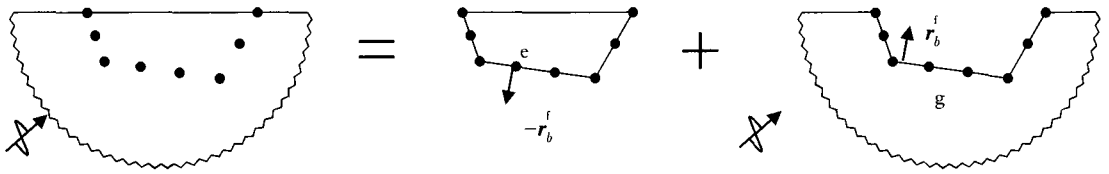

Fig. 2 A half-space under seismic excitation

4 Calculation of soil-structure interaction forces

It is exact but very expensive to evaluate the soil-structure interaction forces directly by convolution integral as shown in Eq. (5), because the computational effort would be proportional to the square of the number of time stations. Moreover, the full sequence of the unit-impulse response matrix of the unbounded soil is required, meaning that the convolution integral and Lyapunov equation must be treated at each time station in SBFE. To reduce the numerical cost, decomposition and truncation of the acceleration unit-impulse response function are performed.

4.1 Decomposition

The second order time derivative of the acceleration unit-impulse response function, denoted by $\ddot{\boldsymbol{G}}^{\mathrm{g}}_{bb}$, is equivalent to the regular part of the displacement unit-impulse response function, which converges to zero physically for an energy dissipation system. In other words, the acceleration unit-impulse response function $\boldsymbol{G}^{\mathrm{g}}_{bb}$ tends essentially to vary linearly. Therefore, $\boldsymbol{G}^{\mathrm{g}}_{bb}$ can be decomposed as shown in Fig. 3

$$\boldsymbol{G}^{\mathrm{g}}_{bb}(t) = \boldsymbol{C}^{\mathrm{g}}_{bb}H(t) + \boldsymbol{K}^{\mathrm{g}}_{bb}tH(t) + \boldsymbol{G}^{\mathrm{m}}_{bb}(t) \tag{6}$$

where $H(t)$ is the Heaviside step function, and the residual function $\boldsymbol{G}^{\mathrm{m}}_{bb}$ converges to zero when time increases to infinity. Thus, Eq. (5) can be rewritten as

$$\boldsymbol{r}_{b}(t) = \boldsymbol{K}^{\mathrm{g}}_{bb}(\boldsymbol{u}_{b}(t) - \boldsymbol{u}^{\mathrm{f}}_{b}(t)) + \boldsymbol{C}^{\mathrm{g}}_{bb}(\dot{\boldsymbol{u}}_{b}(t) - \dot{\boldsymbol{u}}^{\mathrm{f}}_{b}(t)) + \int_0^t \boldsymbol{G}^{\mathrm{m}}_{bb}(t-\tau)(\ddot{\boldsymbol{u}}_{b}(\tau) - \ddot{\boldsymbol{u}}^{\mathrm{f}}_{b}(\tau))\mathrm{d}\tau + \boldsymbol{r}^{\mathrm{f}}_{b}(t) \tag{7}$$

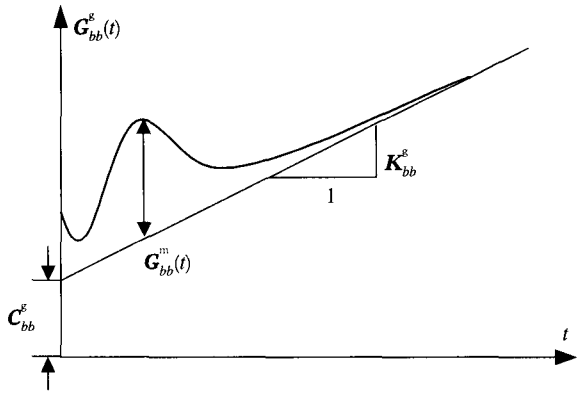

Fig. 3 Decomposition of the acceleration unit-impulse response function

where the static-stiffness coefficient matrix of the unbounded medium $\boldsymbol{K}^{\mathrm{g}}_{bb}$ can be obtained by solving an algebraic Riccati equation, while the damping coefficient matrix $\boldsymbol{C}^{\mathrm{g}}_{bb}$ is evaluated approximately later.

4.2 Truncation

Considering the convergence-to-zero property, $\boldsymbol{G}_{bb}^{\mathrm{m}}$ can be approximated as

$$\boldsymbol{G}_{bb}^{\mathrm{m}}(t) \approx \begin{cases} \boldsymbol{G}_{bb}^{\mathrm{g}}(t) - \boldsymbol{C}_{bb}^{\mathrm{g}} - \boldsymbol{K}_{bb}^{\mathrm{g}} t & 0 \leq t < t_{\mathrm{c}} \\ \boldsymbol{0} & t \geq t_{\mathrm{c}} \end{cases} \tag{8}$$

where t_{c} is called the *cut-off* time.

Whether the truncated function of the unit-impulse response matrix satisfies the prescribed tolerance depends on the cut-off time t_{c}. To determine the cut-off time t_{c}, the following criterion is introduced. In the process of calculatibg the unit-impulse matrix via SBFE with a prescribed tolerance parameter p_{tol}, the normalized Frobenius norm $F(t)/F(0)$, which converges to zero monotonously as will be demonstrated later, is computed at each time station. Once the inequality

$$F(t)/F(0) \leq p_{\mathrm{tol}} \tag{9}$$

is satisfied, the time station is selected to be the *cut-off time* t_{c}.

Consider two typical unbounded media as shown in Fig. 4, and a variation of the normalized Frobenius norms $F(t)/F(0)$ with the dimensionless time $\bar{t} = tc_{\mathrm{p}}/r_0$ plotted in Fig. 5. The property of convergence-to-zero is clearly demonstrated. As can be seen from the figures, with a prescribed value of p_{tol}, the cut-off time depends on the geometry and material property of the unbounded medium.

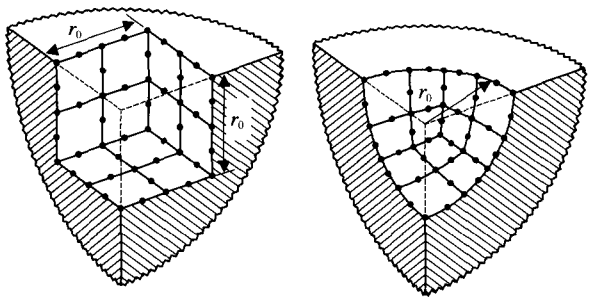

(a) Prismatic excavation (b) Hemi-spherical excavation

Fig. 4 Quarter of a half-space with typical excavation

When t_{c} is determined, the coefficient matrix $\boldsymbol{C}_{bb}^{\mathrm{g}}$ is calculated with $\boldsymbol{K}_{bb}^{\mathrm{g}}$ and the approximate value of $\boldsymbol{G}_{bb}^{\mathrm{g}}$ at t_{c} (see Eq. (8)).

In practical implementation, only a partial sequence of the acceleration unit-impulse response matrix before t_{c} is required. Generally the cut-off time t_{c} is much less than the duration of load history in earthquake engineering, i. e. $t_{\mathrm{c}} << T$, and the enormous numerical cost spent in calculating $\boldsymbol{G}_{bb}^{\mathrm{g}}$ via SBFE is then reduced. Obviously, truncation of the unit-impulse response matrix implies a truncated convolution integral scheme, which allows economical evaluation of the interaction forces.

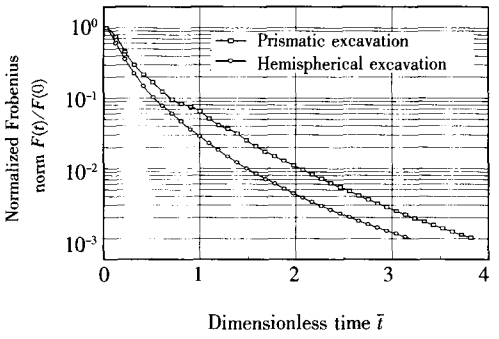

Fig. 5 Variation of the dimensionless Frobenius norms

4.3 Harmonization of time steps

Generally, in calculating the unit-impulse response matrix, a sufficiently small time step, δt (e. g. $10^{-5} \sim 10^{-4}$ s) must be selected in order to accommodate the requirement of computational stability. However, the time step Δt used in the seismic response analysis is usually in the range of $10^{-3} \sim 10^{-2}$ s. The third term on the right hand side of Eq. (7) is rewritten as

$$\boldsymbol{r}_b'(t) = \int_0^t \boldsymbol{G}_{bb}^{\mathrm{m}}(t-\tau)\ddot{\boldsymbol{u}}_b^{\mathrm{a}}(\tau)\mathrm{d}\tau =$$

$$\left(\int_0^{\Delta t} + \int_{\Delta t}^{2\Delta t} + \cdots + \int_{(n-1)\Delta t}^{n\Delta t}\right)\boldsymbol{G}_{bb}^{\mathrm{m}}(t-\tau)\ddot{\boldsymbol{u}}_b^{\mathrm{a}}(\tau)\mathrm{d}\tau \tag{10}$$

where $t = n\Delta t$ and $\ddot{\boldsymbol{u}}_b^{\mathrm{a}} = \ddot{\boldsymbol{u}}_b - \ddot{\boldsymbol{u}}_b^{\mathrm{f}}$. Assuming that the average acceleration as implemented in the Newmark time integral scheme, each term on the right hand side of Eq. (10) can be written as

$$\int_{k\Delta t}^{(k+1)\Delta t} \boldsymbol{G}_{bb}^{\mathrm{m}}(t-\tau)\ddot{\boldsymbol{u}}_b^{\mathrm{a}}(\tau)\mathrm{d}\tau =$$

$$\left(\int_{k\Delta t}^{(k+1)\Delta t} \boldsymbol{G}_{bb}^{\mathrm{m}}(t-\tau)\mathrm{d}\tau\right)\bar{\ddot{\boldsymbol{u}}}_b^{\mathrm{a}}(k\Delta t) \quad k = 0.1, \cdots, n-1 \tag{11}$$

where $\bar{\ddot{\boldsymbol{u}}}_b^{\mathrm{a}}(k\Delta t) = \frac{1}{2}(\ddot{\boldsymbol{u}}_b^{\mathrm{a}}(k\Delta t) + \ddot{\boldsymbol{u}}_b^{\mathrm{a}}((k+1)\Delta t))$.

Then, the discrete form of Eq. (10) is expressed as

$$\boldsymbol{r}_b'(n\Delta t) = \sum_{k=0}^{n-1} \bar{\boldsymbol{G}}_{bb}^{\mathrm{m}}((n-k)\Delta t)\,\bar{\ddot{\boldsymbol{u}}}_b^{\mathrm{a}}(k\Delta t) \tag{12}$$

in which $\bar{\boldsymbol{G}}_{bb}^{m}((n-k)\Delta t)=\int_{k\Delta t}^{(k+1)\Delta t}\boldsymbol{G}_{bb}^{m}(t-\tau)\,d\tau$.

In practical execution, the sequence length of the acceleration unit-impulse response matrix $\boldsymbol{G}_{bb}^{g}$ calculated by SBFE is $t_c/\delta t$, while that of $\bar{\boldsymbol{G}}_{bb}^{m}$ used in evaluating the soil-structure interaction forces is $t_c/\Delta t$. Significant cost reduction could be achieved again.

In this section, no additional approximation is introduced.

5 Final coupling equations

Discretizing Eq.(1) with time step Δt and constituting Eqs. (7) and (12) yield

$$\begin{bmatrix}\boldsymbol{M}_{ss}^{s} & \boldsymbol{M}_{sb}^{s}\\ \boldsymbol{M}_{bs}^{s} & \boldsymbol{M}_{bb}^{s+g}\end{bmatrix}\begin{Bmatrix}\ddot{\boldsymbol{u}}_{s}(n\Delta t)\\ \ddot{\boldsymbol{u}}_{b}(n\Delta t)\end{Bmatrix}+\begin{bmatrix}\boldsymbol{C}_{ss}^{s} & \boldsymbol{C}_{sb}^{s}\\ \boldsymbol{C}_{bs}^{s} & \boldsymbol{C}_{bb}^{s+g}\end{bmatrix}\begin{Bmatrix}\dot{\boldsymbol{u}}_{s}(n\Delta t)\\ \dot{\boldsymbol{u}}_{b}(n\Delta t)\end{Bmatrix}+\begin{bmatrix}\boldsymbol{K}_{ss}^{s} & \boldsymbol{K}_{sb}^{s}\\ \boldsymbol{K}_{bs}^{s} & \boldsymbol{K}_{bb}^{s+g}\end{bmatrix}\begin{Bmatrix}\boldsymbol{u}_{s}(n\Delta t)\\ \boldsymbol{u}_{b}(n\Delta t)\end{Bmatrix}=\begin{Bmatrix}\boldsymbol{p}_{s}(n\Delta t)\\ \boldsymbol{p}_{b}(n\Delta t)\end{Bmatrix} \tag{13}$$

where

$$\boldsymbol{M}_{bb}^{s+g}=\boldsymbol{M}_{bb}^{s}+\boldsymbol{M}_{bb}^{g},\quad \boldsymbol{C}_{bb}^{s+g}=\boldsymbol{C}_{bb}^{s}+\boldsymbol{C}_{bb}^{g},\quad \boldsymbol{K}_{bb}^{s+g}=\boldsymbol{K}_{bb}^{s}+\boldsymbol{K}_{bb}^{g} \tag{14a}$$

$$\begin{aligned}\boldsymbol{P}_{b}(n\Delta t)=&\boldsymbol{M}_{bb}^{g}\ddot{\boldsymbol{u}}_{b}^{f}(n\Delta t)+\boldsymbol{C}_{bb}^{g}\dot{\boldsymbol{u}}_{b}^{f}(n\Delta t)+\\ &\boldsymbol{K}_{bb}^{g}\boldsymbol{u}_{b}^{f}(n\Delta t)-\boldsymbol{r}_{b}^{f}(n\Delta t)-\\ &\sum_{k=0}^{n-2}\bar{\boldsymbol{G}}_{bb}^{m}((n-k)\Delta t)\,\ddot{\bar{\boldsymbol{u}}}_{b}^{a}(k\Delta t)-\\ &\frac{1}{2}\bar{\boldsymbol{G}}_{bb}^{m}(\Delta t)\,\ddot{\boldsymbol{u}}_{b}^{a}((n-1)\Delta t)\end{aligned} \tag{14b}$$

with $\boldsymbol{M}_{bb}^{g}=\frac{1}{2}\bar{\boldsymbol{G}}_{bb}^{m}(\Delta t)$.

As shown in Eq. (13), for the dynamic response of the structure, the effects of unbound soil are characterized by the matrices $\boldsymbol{M}_{bb}^{g}$, $\boldsymbol{C}_{bb}^{g}$ and $\boldsymbol{K}_{bb}^{g}$ (see Eq.(14a)) and the additional external load (see Eq.(14b)). If only external load is considered, Eq. (14b) can be rewritten as

$$\begin{aligned}\boldsymbol{p}_{b}(n\Delta t)=&-\sum_{k=0}^{n-2}\bar{\boldsymbol{G}}_{bb}^{m}((n-k)\Delta t)\,\ddot{\bar{\boldsymbol{u}}}_{bb}^{a}(k\Delta t)-\\ &\frac{1}{2}\bar{\boldsymbol{G}}_{bb}^{m}(\Delta t)\ddot{\boldsymbol{u}}_{b}^{a}((n-1)\Delta t)\end{aligned} \tag{15}$$

6 Numerical examples

The coupling procedure presented in this paper can be applied to the seismic analysis of soil-structure interaction systems directly in time domain. To verify the validity of the present model, the scattering of plane P, SV and SH waves by a hemi-spherical canyon in an elastic isotropic half-space is addressed.

As shown in Fig. 6, the radius of the hemi-spherical canyon is signed by a, a normal vector of wave front is defined in the xOz plane and ϕ is the incident angle.

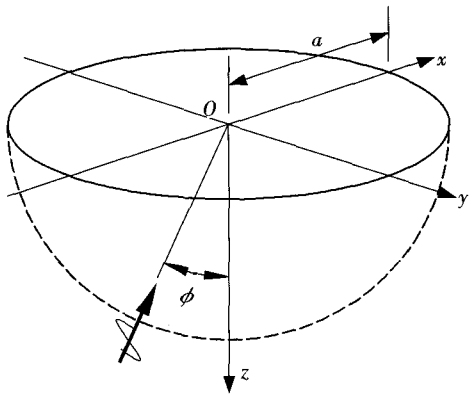

Fig. 6 Hemi-spherical canyon subjected to incident waves

As shown in Fig. 7, a hemi-spherical shell (with thickness 0.273 a) of the soil adjacent to the canyon wall is selected as the structure and discretized by 108 twenty-point hexahedral elements, while the remaining medium is modeled by SBFE. Correspondently, the soil-structure interface is discretized with 108 eight-point quadrangular isoparametric elements. Therefore, there are 1410 degrees of freedom for the entire coupling system, in which 1047 referred to the interface. The excavation is modeled by 216 twenty-point hexahedral elements as pictured in Fig. 8. Poisson's ratio is selected as 0.25 and 1/3 for the P wave and S wave incidence cases, respectively. The seismic analysis time step $\Delta t=0.0005$s is used herein.

The resulting dimensionless amplitude of surface displacement along the x-axis for plane harmonic incident waves are plotted together with those of previous researchers in Figs. 9 to 13, The dimensionless frequencies are defined as $\eta_p=a\omega/\pi c_p$ and $\eta_s=a\omega/\pi c_s$ where c_p and c_s are respectively the dilatational and shear wave velocity, and u, v and w corresponds to the components in the direction of x, y and z, respectively. It is clear that the results from the procedure deseribed herein approach those obtained by Sánche-Sesma and Eshraghi *et al.* when the values of δt and p_{tol} are within the selected range.

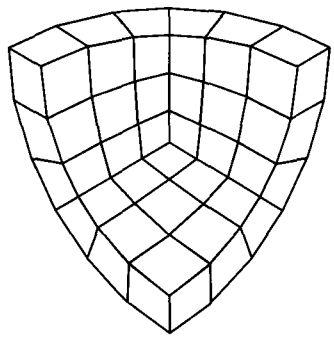

Fig. 7 Finite element mesh of a quarter of structure

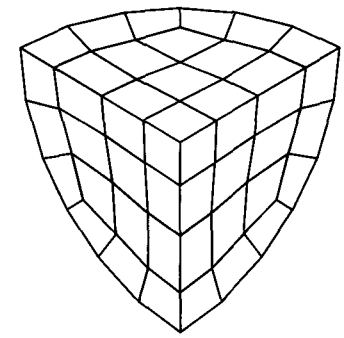

Fig. 8 Finite element mesh of a quarter of excavation

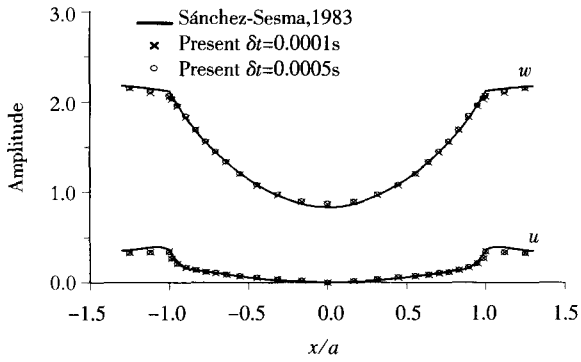

(a) η_p=0.25

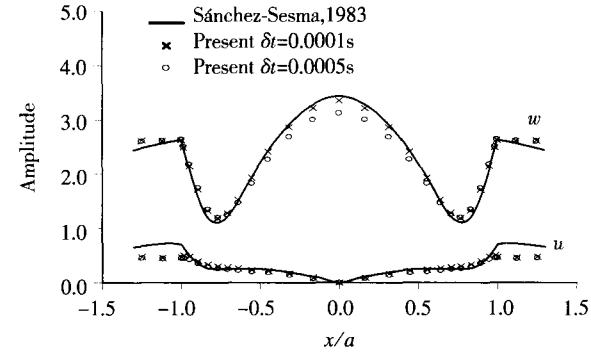

(b) η_p=0.50

Fig. 9 P wave incidence (ϕ=0°, p_{tol}=0.001)

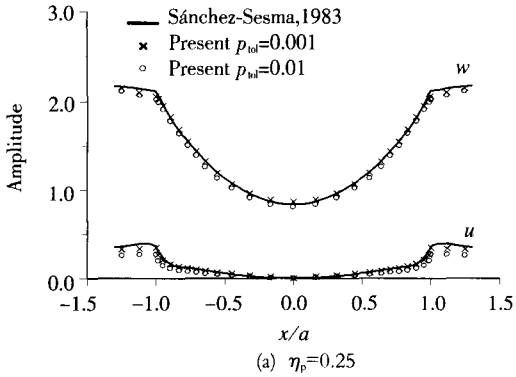

(a) η_p=0.25

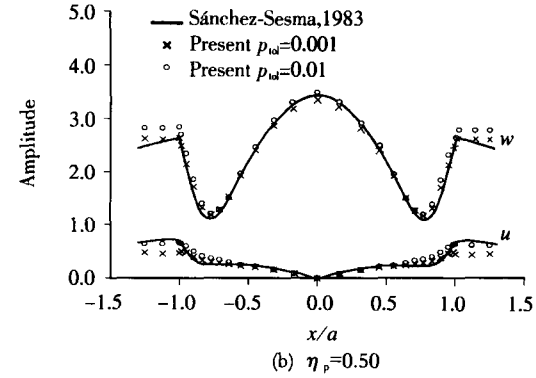

(b) η_p=0.50

Fig. 10 P wave incidence (ϕ=0°, δt=0.0001s)

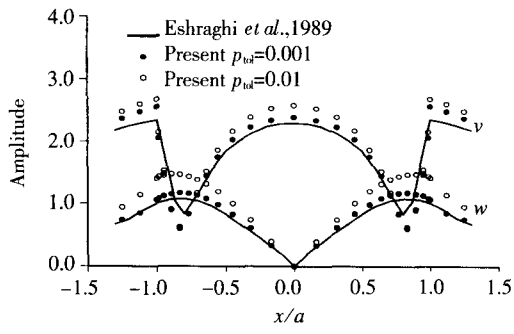

Fig. 11 SV wave incidence (ϕ=0°, η_c=0.75, δt=0.0001s)

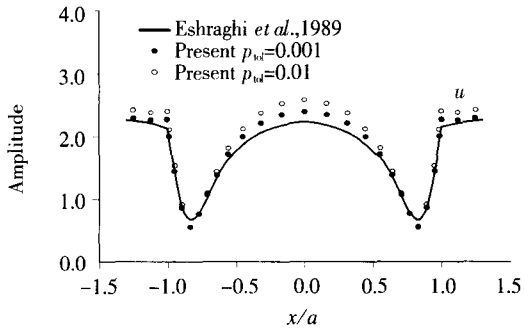

Fig. 12 SH wave incidence (ϕ=0°, η_c=0.75, δt=0.0001s)

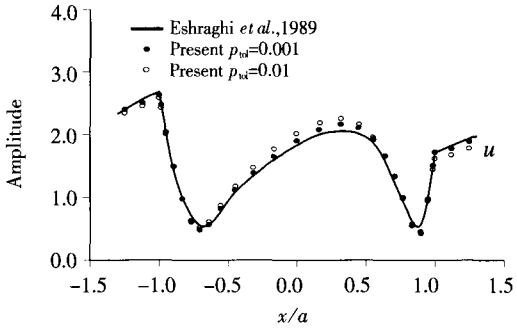

Fig. 13 SH wave incidence (ϕ=30°, η_s=0.75, δt=0.0001s)

It should be noted that the cut-off times t_c for the P and S wave incidence cases are determined as 0.0184s and 0.0175s, respectively, when δt = 0.0001s and P_{tol} = 0.001 are adopted. These values of t_c are very small when compared with actual earthquake time histories, thus the computational effort can be dramatically reduced while also insuring sufficient accuracy.

The sensitivity of the computational accuracy with respect to the selection of time step δt is examined next. In low frequency case, high accuracy can be achieved even if a relatively large value of δt is selected (see Fig. 9(a)), however this is not true in high frequency cases (see Fig. 9(b)). Generally, with the same FE discretization, the input seismic motion of high frequency component can be accurately expressed by using an earthquake time step Δt of 0.0005s. However, this same value does not efficiently represent the local fluctuation of the unit-impulse response function of the unbounded medium. Since the local flucluation would be more important in the high frequency case, large errors could still occur.

The effects of the tolerance parameter p_{tol} on the computational accuracy for two different frequency cases are evaluated. As shown in Fig. 10, the solution to problems under high frequency wave incidence is more sensitive to the selection of p_{tol} than that in low frequency cases. This is due to the fact that the static-stiffness matrix of the unbounded soil $\boldsymbol{K}_{bb}^{g}$ is calculated exactly while the inertial and damping coefficient matrices ($\boldsymbol{M}_{bb}^{g}$ and $\boldsymbol{C}_{bb}^{g}$) are evaluated approximately with a prescribed parameter p_{tol}. It is well known that the low frequency response is mainly controlled by the stiffness of the system while the high frequency response also depends on the inertial and damping properties.

As a consequence, for low frequency dominating problems as encountered in practical seismic analysis, excellent results can be obtained with relative large parameters of δt and p_{tol}, which implies pronounced economy in computational implementation.

7 Conclusions

A seismic free field input formulation is presented for the coupling procedure of FE and SBFE. With a sequence decomposition-truncation implementation and time step harmonization scheme, high efficiency can be achieved. The balance between accuracy and efficiency can be controlled by the prescribed parameter. Validity of the model is verified by numerical examples. The coupling procedure proposed here can be applied to the dynamic response of unbounded soil-structure interaction of large scale systems in time domain. The procedure proposed is especially economical in low frequency dominating systems as frequently encountered in practical seismic analysis.

References

Dasgupta G (1982), "A Finite Element Formulation for Unbounded Homogeneous Continua," *Journal of Applied Mechanics*, ASME, **49**(1): 136-140.

Ekevid T and Wiberg N-E (2002), "Wave Propagation Related to High-Speed Train - a Scaled Boundary FE-approach for Unbounded Domains," *Computer Methods in Applied Mechanics and Engineering*, **191**(36): 3947-3964.

Eringen AC and Suhubi ES (1974), *Elastodynamics*, Academic Press, New York.

Eshraghi H and Dravinski M (1989), "Scattering of Plane Harmonic SH, SV, P and Rayleigh Waves by Non-axisymmetric Three-dimensional Canyons: A Wave Function Expansion Approach," *Earthquake Engineering & Structural Dynamics*, **18**(7): 983-998.

Genes MC and Kocak S (2002), "A Combined Finite Element Based Soil-Structure Interaction Model for Large-scale Systems and Applications on Parallel Platforms," *Engineering Structures*, **24**(9): 1119-1131.

Sánchez-Sesma FJ (1983), "Diffraction of Elastic Waves by Three-dimensional Surface Irregularities," *Bulletin of Seismological Society of America*, **73**(6): 1621-1636.

Song Ch and Wolf JP (1995), "Unit-impulse Response Matrix of Unbounded Medium by Finite-element Based Forecasting," *International Journal for Numerical Methods in Engineering*, **38**(7): 1073-1086.

Song Ch and Wolf JP (1997), "The Scaled Boundary

Finite-element Method - Alias Consistent Infinitesimal Finite-element Cell Method - for Elastodynamics," *Computer Methods in Applied Mechanics and Engineering*, **147**(3-4):329-355.

Wolf JP and Weber B (1982), "On Calculating the Dynamic-Stiffness Matrix of the Unbounded Soil by Cloning," *International Symposium on Numerical Models in Geomechanics*, Zurich, Switzerland, pp. 486-494.

Wolf JP (1985), *Dynamic Soil-Structure Interaction*, Prentice-Hall, Englewood Cliffs, N. J.

Wolf JP and Song Ch (1994), "Dynamic-stiffness Matrix of Unbounded Soil by Finite-element Multi-cell Cloning," *Earthquake Engineering & Structural Dynamics*, **23**(3): 233-250.

Wolf JP and Song Ch (1994), "Dynamic-stiffness Matrix in Time Domain of Unbounded Medium by Infinitesimal Finite Element Cell Method," *Earthquake Engineering & Structural Dynamics*, **23**(11): 1181-1198.

Wolf JP and Song Ch (1996), *Finite-element Modeling of Unbounded Media*, Wiley, New York.

Yan Junyi, Jin Feng and Zhang Chuhan (2002), "A Coupling Procedure of FE and SBFE for Soil-Structure Interaction in Time Domain," *Proceedings of the 3rd International Conference on Boundary Element Techniques*, Beijing, China, pp. 7-13.

Yan Junyi, Jin Feng and Zhang Chuhan (to appear in 2003), "A time domain coupling procedure of FE and SBFE based on linear system theory," *Journal of Tsinghua University Science and Technology*.

Zhang Xiong, Wegner JL and Haddow JB (1999), "Three-dimensional Dynamic Soil-structure Interaction Analysis in the Time Domain," *Earthquake Engineering & Structural Dynamics*, **28**(12): 1501-1524.